Torus Breakdown in Noninvertible Maps

Maistrenko, V.; Maistrenko, Yu.; Mosekilde, Erik

Published in:
Physical Review E. Statistical, Nonlinear, and Soft Matter Physics

Link to article, DOI:
10.1103/PhysRevE.67.046215

Publication date:
2003

Document Version
Publisher's PDF, also known as Version of record

Torus breakdown in noninvertible maps

V. Maistrenko* and Yu. Maistrenko
Institute of Mathematics, National Academy of Sciences of Ukraine, Kiev 252601, Ukraine

E. Mosekilde
Department of Physics, The Technical University of Denmark, 2800 Kgs. Lyngby, Denmark
(Received 13 November 2002; published 24 April 2003)

We propose a criterion for the destruction of a two-dimensional torus through the formation of an infinite set of cusp points on the closed invariant curves defining the resonance torus. This mechanism is specific to noninvertible maps. The cusp points arise when the tangent to the torus at the point of intersection with the critical curve L_0 coincides with the eigendirection corresponding to vanishing eigenvalue for the noninvertible map. Further parameter changes lead typically to the generation of loops (self-intersections of the invariant manifolds) followed by the transformation of the torus into a complex chaotic set.

DOI: 10.1103/PhysRevE.67.046215 PACS number(s): 05.45.Xt

I. INTRODUCTION

Torus destruction through the loss of smoothness is a common phenomenon in systems that display quasiperiodicity and phase locking [1]. Together with the period doubling and intermittency transitions, torus destruction represents one of the classical routes to chaos in dissipative systems, and torus destruction has attracted considerable interest in connection with studies of the onset of turbulence [2]. Examples of torus destruction have also been described for coupled (or forced) oscillator systems in physics [3], biology [4,5], and other fields of science [6,7].

In their seminal paper on the breakdown of two-dimensional tori, Afraimovich and Shilnikov [8] outlined three possible scenarios for the destruction of a torus arising as a Poincaré section of a quasiperiodic flow. In all scenarios, the starting point is a smooth torus in a resonance region where a stable periodic orbit (node) coexists with an unstable orbit (saddle cycle) of the same periodicity. The torus itself is defined as the closure of the unstable manifolds of the saddle cycle with the points of the saddle and stable node. In one scenario, the unstable manifolds from the saddle cycle start to develop wrinkles as they approach the points of the stable node. In this way, the torus becomes nondifferentiable in these points. As the system, under variation of a parameter, leaves the resonance zone, wrinkles and nonsmoothness spread along the invariant manifolds, and the torus breaks up into a fractal structure.

In another scenario, the unstable manifolds from the saddle cycle start to intersect the nonleading manifolds of the node. This produces an infinitely folded structure accumulating at the node points, where the torus again loses its smoothness. The torus is destructed when this folded structure makes contact with the stable manifold of the same saddle cycle in a homoclinic tangency. Finally, in the third scenario, the stable node is transformed into a stable focus and the unstable manifolds from the saddle cycle start to spiral around the focus points. The focus subsequently undergoes a Hopf bifurcation or a sequence of period doublings. The consistency of these scenarios has been tested in several numerical studies, e.g., by Curry and Yorke [9] and by Aronson *et al.* [10]. It has also been shown that torus destruction can take place through a crisis involving the collision with its basin boundary [11].

The torus destruction scenarios apply to smooth systems and to systems that can be represented by two-dimensional invertible maps. For nonsmooth systems, modifications arise in connection with the occurrence of so-called border collision bifurcations by which, for example, the transformation of a node into a focus can occur abruptly [12]. The purpose of this paper is to describe a mechanism that is specific to noninvertible maps where the invariant manifold defining the torus can intersect itself. This gives rise to cusp points followed by the transition to a characteristic loop structure that cannot occur for invertible maps. We show how the self-intersection mechanism can operate in conjunction with the invertible mechanisms described by Afraimovich and Shilnikov and establish the criterion for the self-intersections of the invariant manifolds to emerge.

Noninvertible two-dimensional maps arise, for instance, in the study of chaotic synchronization [13]. Evidence of a loop structure of the invariant manifold was also observed by Lorenz [14] in a study of computational chaos, by Anishchenko *et al.* [15] in a study of the destruction of three-dimensional tori in a periodically forced system of two coupled logistic maps, and by Frouzakis *et al.* [16] in a study of a model-reference, self-adapting control system. A preliminary investigation of the mechanisms for torus destruction of noninvertible maps was also reported by Maistrenko *et al.* [17].

In the case of noninvertible maps $F:\mathbb{R}^2\to\mathbb{R}^2$, we find that a new bifurcation can take place after the torus has become nonsmooth and before it is destroyed. Let us illustrate this transition for a situation that corresponds to the first of the above mentioned scenarios (wrinkled route to destruction). As shown in Fig. 1(a), the resonance torus T_r loses its smoothness at the point P_m of the stable node due to folding of the unstable manifold $W_Q^{(u)}$ that connects the saddle Q_m to the node P_m. The first folding [indicated by an asterisk in

*Electronic address: maistren@nas.gov.ua

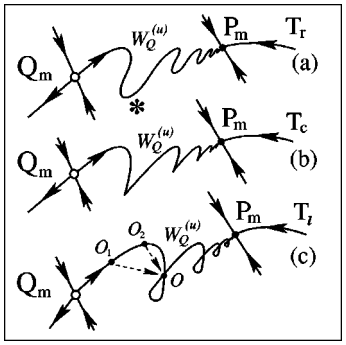

FIG. 1. Schematic representation of the transition from a nonsmooth resonance torus T_r via a cusp torus T_c to a loop torus T_l. $W_Q^{(u)}$ represents the unstable manifold from the saddle point Q_m toward the node point P_m. The first point O of self-intersection of $W_Q^{(u)}$ must have two different preimages O_1 and O_2 both belonging to T_l.

Fig. 1(a)] is repeated indefinitely as the manifold approaches P_m, with the scales of the successive foldings decreasing in accordance with the eigenvalues of P_m.

If the map is noninvertible, the further evolution of the unstable manifold $W_Q^{(u)}$ can give rise to the appearance of cusp points [Fig. 1(b)] followed by the formation of loops [Fig. 1(c)]. We find that the cusp points arise when the tangent of the unstable manifold $W_Q^{(u)}$ at the point of intersection with the critical curve L_0 coincides with the eigendirection of vanishing eigenvalue for F. We conclude that there can be two new characteristic shapes for a torus in the case of noninvertible maps: the cusp torus T_c [Fig. 1(b)] and the loop torus T_l [Fig. 1(c)]. Note that the topological structure of the loop torus T_l is different from that of a circle. Indeed, T_l is no longer homeomorphic to a circle but endomorphic only to it. For the loop torus T_l, the first intersection point $O \in T_l$ must have two preimages $O_1 \neq O_2$ belonging to T_l. Therefore, the restriction F_T of the map F to the torus T_l is also noninvertible. Moreover, we conclude that the transition from T_r to T_l happens just at the moment when the map F_T on the torus T_r becomes noninvertible.

With further parameter variation, the loop torus T_l can be destroyed in accordance with scenarios analogous to those of the invertible case.

II. CUSP AND LOOP TORI FOR NONINVERTIBLE MAPS

Let us illustrate the sequence of torus bifurcations for two-dimensional, noninvertible maps by means of the model

$$x_{n+1} = f(x_n) + \varepsilon[f(y_n) - f(x_n)]$$

$$y_{n+1} = f(y_n) + \varepsilon[f(x_n) - f(y_n)], \qquad (1)$$

of two coupled logistic maps. Here the one-dimensional map $f = f_a = ax(1-x)$, $x \in [0,1], 0 \leq a \leq 4$, with $n = 0,1,\ldots$ denoting a discrete time variable. The two-dimensional map F defined by Eq. (1) has two parameters, of which a controls the nonlinearity of the logistic map and ε is the coupling parameter.

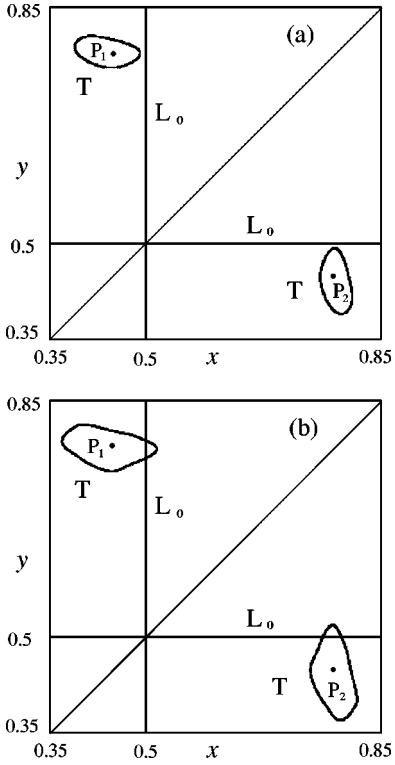

FIG. 2. Phase portraits for the recurrent map system (1) with a coupling parameter $\varepsilon = 1.285$ (a) and $\varepsilon = 1.300$ (b). In both figures, the nonlinearity parameter $a = 2.95$. In (b) the symmetric tori T intersect the critical lines L_0 at which the Jacobian determinant of the map vanishes.

The recurrent map system (1) as well as various generalizations have been intensively studied in the past years [18,19]. In particular, maps of this type have been used in the study of chaotic synchronization [13] and clustering [20]. It was observed in these studies that after the riddling and blowout bifurcations of the chaotic synchronous state, the dynamics of the coupled map system (1) typically develops through an Andronov-Hopf bifurcation of an asymmetric cycle P, giving rise to a stable invariant curve, i.e., a torus T [Fig. 2(a)], which then transforms into a resonance torus T_r. In Fig. 2(a), the torus T does not yet intersect the critical lines L_0 of the map F, while in Fig. 2(b) such an intersection has occurred.

By a critical line L_0 of the map F, we mean a curve in phase space where the Jacobian determinant vanishes,

$$|DF| = 0.$$

The concept of critical curves for two-dimensional noninvertible maps and the role that the iterates of these curves play in delineating the so-called absorbing area (and, hence, the chaotic attractor) were introduced and extensively applied by Gumowski and Mira [21] and by Mira *et al.* [22,23]. Critical curves represent a generalization of the well-known concept of critical points for one-dimensional noninvertible maps, i.e., points at which the map has vanishing slope and where the number of preimages suddenly changes.

For the considered map F of the form (1), the Jacobian determinant vanishes at two perpendicular lines $x=0.5$ and $y=0.5$. Hence, the critical curves L_0 are found as (see Fig. 2)

$$L_0=\{x=0.5\}\cup\{y=0.5\}.$$

Moreover, while the position of the cycle P and the diameter of the torus T depend on a and ε, the critical lines are independent of these parameters.

The resonant torus T_r in Fig. 2(b), although it intersects the critical line L_0, is still associated with an invertible dynamics: the mapping F_T along the torus T is one to one. With further parameter variation, F_T becomes noninvertible. This happens when the tangent to the torus T in the point of intersection with the critical line L_0 coincides with the direction of vanishing eigenvalue for F. Due to the symmetry of F with respect to the diagonal, we need to consider only one torus T [e.g., the right-hand side of Fig. 2(b)]. This torus intersects the horizontal part of L_0. It is easy to show that the eigenvectors corresponding to the zero eigenvalue of the map F at the critical line L_0 are vertical. Hence, we conclude that cusp points on the torus arise (the cusp torus T_c appears) when the tangent to the torus at the point of intersection with L_0 becomes vertical.

Figure 3 shows the main stages in this transformation. Here, $a=3.86$ while the coupling parameter is changed from $\varepsilon=0.904\,48$ (a) over $\varepsilon=0.904\,52$ (b) to $\varepsilon=0.904\,55$ (c). With these parameter values, we are operating in a resonance zone with a stable period-15 node and a saddle cycle of the same periodicity. This region of operation was chosen because the point P of the node falls very close to the critical line L_0. This allows us to follow the loop formation in real (i.e., undistorted) scale.

As before, $W_Q^{(u)}$ denotes the unstable manifold of the saddle cycle. $\vec{u}$ represents the normal to the critical line L_0 and $\vec{k}$ is the tangent to $W_Q^{(u)}$ in the point of intersection between L_0 and $W_Q^{(u)}$. In Fig. 3(a), $W_Q^{(u)}$ is folded such that the torus is already nonsmooth at the point P. However, $W_Q^{(u)}$ intersects L_0 in such a direction that the dynamics along $W_Q^{(u)}$ is invertible. In Fig. 3(b), $\vec{k}$ has become vertical and now coincides with the direction of vanishing eigenvalue for F. This is the moment of formation for the cusp torus T_c. Now the unstable manifold has acquired an infinite number of nonsmooth points. Finally, in Fig. 3(c), the angle α has changed sign, the dynamics along $W_Q^{(u)}$ is no longer invertible, and an infinite sequence of loops has developed along the manifold. Hence, we have observed how the transformation proceeds through the following steps:

$$T_r \Rightarrow T_{cusp} \Rightarrow T_{loop}. \tag{2}$$

Figure 4 illustrates the bifurcation sequence in the case when the point P is a focus, i.e., the resonance torus T_r has lost its smoothness with the eigenvalues of P becoming complex.

We are still considering a resonance zone with a period-15 cycle. For $a=3.867\,85$ and $\varepsilon=0.903\,25$ [Fig. 4(a)], the torus

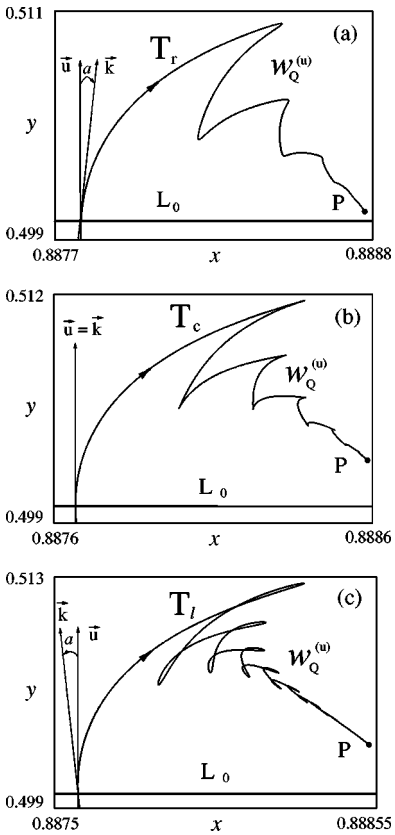

FIG. 3. Transition from a nonsmooth resonance torus T_r via a cusp torus T_c to a loop torus T_l for the case when the stable cycle is a node. $a=3.86$. The coupling parameter is changed from $\varepsilon=0.904\,48$ (a) over $\varepsilon=0.904\,52$ (b) to $\varepsilon=0.904\,55$ (c). The cusp torus T_c arises when the unstable manifold $W_Q^{(u)}$ intersects the critical line L_0 perpendicularly.

is smooth, except in the points of the focus. At the moment when the unstable manifold $W_Q^{(u)}$ intersects the critical line L_0 perpendicularly, the unstable manifold develops an infinite set of cusp points [Fig. 4(b)], and when the angle α between $\vec{u}$ and $\vec{k}$ changes sign, a loop torus T_l develops [Fig. 4(c)].

III. TRANSITION TO CHAOS

As noted in the Introduction, torus breakdown represents one of the three classic routes to chaos in dissipative systems. Let us therefore follow the development of a loop torus as the system leaves the resonance zone.

To illustrate this transition, we have chosen to consider a somewhat different region of parameter space where we find a resonance torus with period-5 dynamics. The reason for this choice is that, in the examples we will consider, the transition to chaos maintains the looplike structure whose mechanism of creation was explained in Sec. II.

Figure 5 provides an overview of the relevant part of the parameter space. In the lower left corner (gray shaded region), the two-dimensional map (1) displays a stable asymmetric fixed point (actually, of course, two mutually symmetric fixed points as illustrated in Fig. 2). At the transition to the unshaded zone, the fixed point undergoes an Andronov-Hopf bifurcation for maps, and for parameter combinations

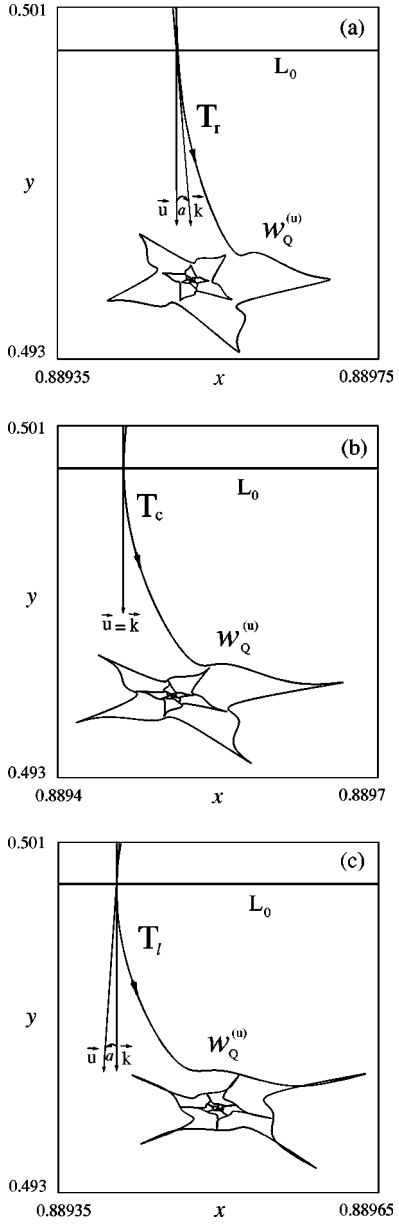

FIG. 4. Transition from a nonsmooth resonance torus T_r via a cusp torus T_c to a loop torus T_l for the case when the stable cycle is a focus. Here $a=3.867\,85$ and $\varepsilon=0.903\,25$ (a), $a=3.867\,90$ and $\varepsilon=0.903\,25$ (b), $a=3.868\,00$ and $\varepsilon=0.903\,45$ (c).

to the right of this bifurcation curve, we observe quasiperiodic dynamics (on an ergodic torus) followed by resonant behavior and chaos. Curves 1 and 2 delineate the region of period-5 resonant dynamics. In the lower part of this tongue (below the doted curve), the stable period-5 cycle at the torus is a node. Above the dotted curve, the period-5 cycle is a focus. Finally, the focus loses stability in an Andronov-Hopf bifurcation at curve 3. Above this curve, another region of quasiperiodic dynamics can be found as well as resonance zones, including a region with period-15 dynamics.

Figure 6 demonstrates the rapid variation of the largest Lyapunov exponent λ_1 that takes place as the system leaves the period-5 resonance zone, starting from point *A* (see Fig. 5) at $\varepsilon=1.54$ and $a=2.766$ in the direction of the arrow. To

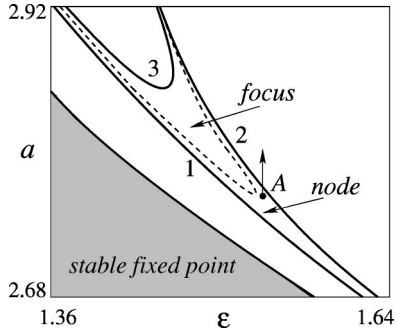

FIG. 5. Two-dimensional bifurcation diagram for the coupled map system (1). The curves 1 and 2 delineate a region with period-5 resonance behavior. At the dotted curve, the stable period-5 cycle is transformed from a node into a focus. Curve 3 is an Andronov-Hopf bifurcation curve for the period-5 orbit.

the left in the figure, the coupled map system displays a resonance torus with loops and λ_1 is negative. When *a* is increased, transitions between periodic ($\lambda_1<0$), quasiperiodic ($\lambda_1=0$) and chaotic ($\lambda_1>0$) dynamics occur extremely fast. The second Lyapunov exponent λ_2 remains negative.

Figure 7 illustrates the changes of the stationary solution to Eq. (1) that take place as the system leaves the resonance tongue in the direction of the arrow from point *A* in Fig. 5. In Fig. 7(a), we still have the characteristic structure of a loop torus. As before, *P* represents the stable node, and $W_Q^{(u)}$ is the unstable manifold that approaches *P* from the saddle cycle (not shown). Here $a=2.766$ and $\varepsilon=1.54$. In Fig. 7(b), $a=2.7738$ and $\varepsilon=1.533\,85$. It is interesting to note that how the overall structure of the loop torus is maintained as the loop is broken and the system becomes chaotic. For the parameters of this figure, the Lyapunov exponents are $\lambda_1\cong 0.0145$ and $\lambda_2\cong -0.028$. Hence, the Lyapunov dimension $D_L\cong 1.52$. In Fig. 7(c), the system has moved a little further out of the resonance tongue. With $a=2.774$ and $\varepsilon=1.5339$, we now have $\lambda_1\cong 0.013$, $\lambda_2\cong -0.021$, and $D_L\cong 1.62$. Initial conditions are always chosen in a neighborhood of *CA*.

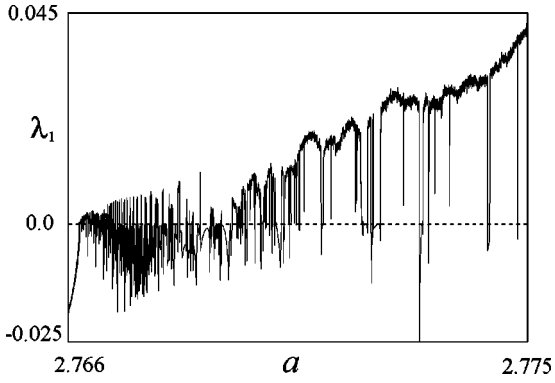

FIG. 6. Variation of the largest Lyapunov exponent λ_1 with the nonlinearity parameter *a*. The coupled map system leaves the period-5 Arnol'd tongue at $a\cong 2.7662$. Note the extremely rapid transition between periodic ($\lambda_1<0$), quasiperiodic ($\lambda_1=0$), and chaotic ($\lambda_1>0$) dynamics immediately outside the tongue. $\varepsilon=1.54$.

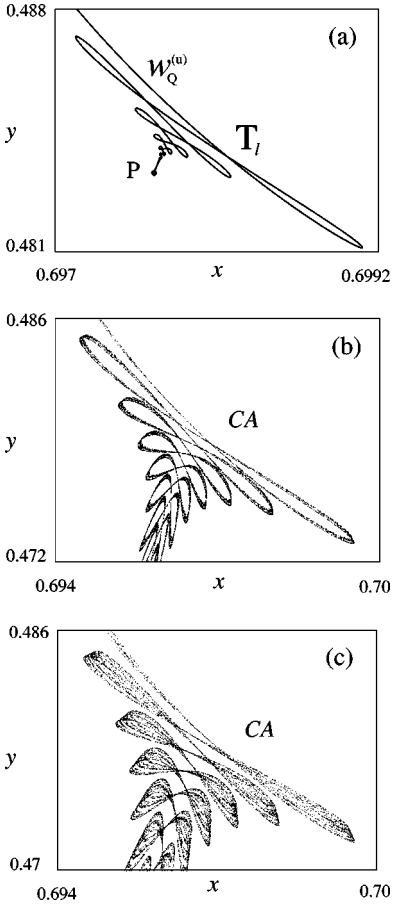

FIG. 7. Transition from loop torus T_l to chaotic attractor CA as the system passes out through the period-5 Arnol'd tongue in the direction of the arrow from point A of Fig. 5. $a=2.7660$, $\varepsilon=1.54$ (a), $a=2.7738$, $\varepsilon=1.53385$ (b), and $a=2.7740$, $\varepsilon=1.5339$ (c). Note how the characteristic loop structure is maintained in the initial stages of the torus breakdown.

Figure 8 presents a picture of the full chaotic attractor CA for $a=2.774$ and $\varepsilon=1.535$. Although the Lyapunov dimension now is $D_L\cong 2.0$, one can easily observe the signatures both of the original period-5 node and of the self-intersecting manifolds of the resonance torus. Figure 8(b) is a magnification of the part of the chaotic attractor, corresponding to the region delineated by the dotted square in Fig. 8(a).

IV. CONCLUSION

Gumowski and Mira [21] and Mira *et al.* [22,23] have developed the concept of critical curves for two-dimensional noninvertible maps and discussed the bifurcations of invariant manifolds in connection with their self-intersections. We used these ideas to establish the precise criterion for the loop structure to arise and to illustrate how the loop formation mechanism works in conjunction with the classic Afraimovich-Shilnikov scenarios of torus breakdown. It was possible to clearly distinguish the processes that are associated with the lack of invertibility for the map. In particular, an additional bifurcation (in which the closed invariant curve develops an infinite set of cusp points and then loops) could be identified between the transition in which the invariant curve becomes nonsmooth and its final breakdown.

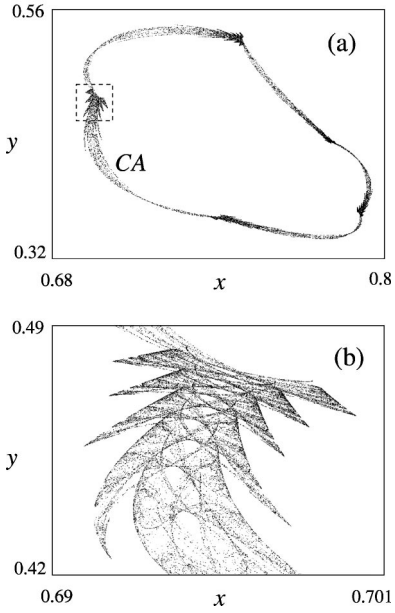

FIG. 8. Fully formed chaotic attractor CA outside the period-5 Arnol'd tongue (a). The Lyapunov dimension is now $D_L\cong 2.0$. One can still observe the signatures of the period-5 resonance dynamics and of the self-intersecting manifolds. Magnification of part of (a) (b). Parameter values are $a=2.774$, $\varepsilon=1.535$.

To simplify the discussion, we considered a system of two nonlinearly coupled logistic map. Here, the critical curves are two straight lines, perpendicular to one another. In the general case, the mapping $F:\mathbb{R}^2\to\mathbb{R}^2$ may be represented as

$$\begin{pmatrix} x \\ y \end{pmatrix} \mapsto \begin{pmatrix} u(x,y) \\ v(x,y) \end{pmatrix},$$

with $u\in C^1$ and $v\in C^1$. The function F has partial derivatives $u'_x(x,y)$, $u'_y(x,y)$, $v'_x(x,y)$, and $v'_y(x,y)$ in all points. However, if F is noninvertible, it has a direction of vanishing derivative along a critical curves L_0 where the Jacobian determinant $DF=0$.

When the invariant manifold of a saddle cycle crosses the critical curve in the direction of vanishing derivative for F, an infinite set of cusp points arise. As the parameters of the system are changed, the cusp points develop typically into loop points, and the closed invariant curve will no longer be homeomorphic to a circle.

We have demonstrated how this loop structure arises in connection with two of the Afraimovich-Shilnikov scenarios, i.e., in connection with the developments of both wrinkles and spirals on the invariant manifold. We have also shown how this loop structure partly survives as the torus starts to break up.

ACKNOWLEDGMENTS

We thank L.P. Shilnikov for a number of illuminating discussions. V. and Yu. Maistrenko acknowledge financial support from Danish Graduate School in Nonlinear Science.

[1] V. Franceschini, Physica D **6**, 285 (1983); S. Ostlund, D. Rand, J. Sethna, and E. Siggia, *ibid.* **8**, 303 (1983); M. Sano and Y. Sawada, Phys. Lett. A **97**, 73 (1983).

[2] D. Ruelle and F. Takens, Commun. Math. Phys. **20**, 167 (1971); J.P. Gullub and S.V. Benson, J. Fluid Mech. **100**, 449 (1980); J. Stavans, F. Heslot, and A. Libchaber, Phys. Rev. Lett. **55**, 596 (1985).

[3] V.S. Anishchenko and T.E. Letchford, Sov. Phys. Tech. Phys. **31**, 1347 (1986); E. Mosekilde, R. Feldberg, C. Knudsen, and M. Hindsholm, Phys. Rev. B **41**, 2298 (1990).

[4] H. Hayashi, M. Nakao, and K. Hirakawa, Phys. Lett. A **88**, 265 (1982); L. Glass, M.R. Guevara, A. Shrier, and R. Perez, Physica D **7**, 89 (1983).

[5] G. Baier, J.S. Thomsen, and E. Mosekilde, J. Theor. Biol. **165**, 593 (1993).

[6] T. Matsumoto, L.O. Chua, and R. Tokunaga, IEEE Trans. Circ. Syst. CAS **34**, 240 (1987); V.S. Anishchenko, M.A. Safonova, and L.O. Chua, *ibid.* **40**, 792 (1993).

[7] C.B. Sørensen, E. Mosekilde, and P. Gránásy, Phys. Scr., T **T67**, 176 (1996).

[8] V.S. Afraimovich and L.P. Shilnikov, Am. Math. Soc. Trans. **149**, 201 (1991); V.I. Arnol'd, V.S. Afraimovich, Yu. S. Il'Yashenko, and L.P. Shilnikov, *Dynamical Systems* (Springer, Berlin, 1991), Vol. V.

[9] J. Curry and J.A. Yorke, *The Structure of Attractors in Dynamical Systems*, Lecture Notes in Mathematics Vol. 668 (Springer, Berlin, 1977), p. 48.

[10] D.G. Aronson, M.A. Chory, G.R. Hall, and R.P. McGhee, Commun. Math. Phys. **83**, 303 (1982).

[11] C. Letellier, A. Dinklage, H. El-Naggar, C. Wilke, and G. Bonhomme, Phys. Rev. E **63**, 042702 (2001).

[12] Zh.T. Zhusubaliyev, E.A. Soukhoterin, and E. Mosekilde, Chaos, Solitons Fractals **13**, 1889 (2002).

[13] Yu. Maistrenko, V. Maistrenko, O. Popovych, and E. Mosekilde, Phys. Lett. A **262**, 355 (1999); Phys. Rev. E **60**, 2817 (1999); A.V. Taborov, Yu. Maistrenko, and E. Mosekilde, Int. J. Bifurcation Chaos Appl. Sci. Eng. **10**, 1051 (2001); E. Mosekilde, Yu. Maistrenko, and D. Postnov, *Chaotic Synchronization Application to Living Systems* (World Scientific, Singapore, 2002).

[14] E.N. Lorenz, Physica D **35**, 299 (1989).

[15] V.S. Anishchenko, M.A. Safonova, U. Feudel, and J. Kurths, Int. J. Bifurcation Chaos Appl. Sci. Eng. **4**, 595 (1994).

[16] C.E. Frouzakis, R.A. Adomaitis, and I.G. Kevrekidis, Int. J. Bifurcation Chaos Appl. Sci. Eng. **1**, 83 (1991).

[17] V. Maistrenko, Yu. Maistrenko, and I. Sushko, Int. J. Bifurcation Chaos Appl. Sci. Eng. **4**, 383 (1994).

[18] J. Frøyland, Physica D **8**, 432 (1983); C. Reick and E. Mosekilde, Phys. Rev. E **52**, 1418 (1995).

[19] L. Gardini, R. Abraham, R. Record, and D. Fournier-Prunaret, Int. J. Bifurcation Chaos Appl. Sci. Eng. **4**, 145 (1994); C.E. Frouzakis, L. Gardini, I.G. Kevrekidis, G. Millerioux, and C. Mira, *ibid.* **7**, 1167 (1997).

[20] O. Popovych, Yu. Maistrenko, and E. Mosekilde, Phys. Rev. E **64**, 026205 (2001); Phys. Lett. A **302**, 171 (2002).

[21] I. Gumowski and C. Mira, *Recurrence and Discrete Dynamical Systems*, Lecture Notes in Mathematics Vol. 809 (Springer, Berlin, 1980).

[22] C. Mira and T. Narayaninsamy, Int. J. Bifurcation Chaos Appl. Sci. Eng. **3**, 187 (1993).

[23] C. Mira, L. Gardini, A. Barugola, and J.-C. Cathala, *Chaotic Dynamics in Two-Dimensional Noninvertible Maps* (World Scientific, Singapore, 1996).